7B.1

STATISTICAL EVALUATION OF PULSE TO PULSE PHASE CODING TO SUPPRESS COUPLING IN THE POLARIMETRIC RADAR

Igor R. Ivić[(1)(2)], and Dušan S. Zrnić[(1)]
(1) Cooperative Institute for Mesoscale Meteorological Studies (CIMMS), The University of Oklahoma
(2) NOAA/OAR National Severe Storms Laboratory, Norman, Oklahoma

1. INTRODUCTION

Currently, the weather surveillance radar-1988 Doppler (WSR-88D), operated by the National Weather Service, is one of the key providers of weather information for the entire nation. As such, the WSR-88D network is constantly evolving. The most recent and significant addition to the network is the dual-polarization capability. Dual polarization introduces new information that improves the abilities of forecasters and algorithms to distinguish between different types of precipitation (e.g., rain, hail) and non-weather scatterers (e.g., insects, ground clutter).

In the recent years, phased array radar (PAR) technology has been proposed as foundation for development of the next generation of weather surveillance systems. This technology supports more flexible scanning strategies than radars using mechanically steered antennas and has the potential to provide reduced data update times. Advantages of using PAR technology for weather observations are discussed by Zrnić at al. (2007), and experiments demonstrating these using a single-polarized PAR are conducted at the National Severe Storms Lab (e.g., Heinselman and Torres 2011). PAR technology has been principally developed to advance point target detection and tracking; hence, dual-polarization has not been widely implemented on such systems. It is clear, though, that weather radars of the next generation will have to combine PAR and dual-polarization technology to meet and exceed the current weather surveillance capabilities.

Generally, implementation of dual-polarization for weather applications imposes strict requirements on antenna design and fabrication. This is due to the nature of dual-polarization measurements which require considerable isolation between horizontal and vertical channels. Namely, the close proximity of hardware and imperfections in fabrication cause a portion of the energy transmitted in the horizontal (H) channel to leak into the vertical (V) channel, and vice versa. In addition, the same effect is present on reception too. The result is that the measured voltages are contaminated by leakage between the H and V channels. The dual-polarization measurement that are susceptible to this problem are the differential reflectivity (Z_{DR}) because it is computed from the ratio of returned powers in the two orthogonal channels and the copolar correlation coefficient. Due to the nature of planar phased arrays, coupling through hardware (especially the antenna) is even more prominent compared to a reflector antenna. Additionally, a PAR can form thousands of beams, each of which may have varying gain, beam width, and polarimetric characteristics. Furthermore, in some architectures, non-orthogonal orientation of intended H and V fields occurs when the beam is pointed in directions that are not perpendicular to the array (i.e., away from the principal planes) (Zhang et al. 2009). To overcome this particular problem Zhang et al. (2011) proposed a cylindrical design whereby the beam is steered in azimuth by commuting illumination of the radiators so that beams are always in the vertical principal plane. Another alternative is a system where beams are electronically scanned only in the orthogonal principal planes (Knapp et al. 2011). Nonetheless, even with these solutions cross-polar coupling through the radar antenna and surrounding microwave circuitry remain and must be dealt with.

Two dual-polarization transmission schemes have been proposed. In the AHV mode, H and V fields are alternately transmitted, whereas in the SHV mode fields are transmitted simultaneously. For the same cross-polar isolation, the AHV mode has the advantage that the Z_{DR} bias is much smaller than in the SHV mode (Sachidananda and Zrnić 1985)). Unfortunately, the AHV mode of operation presents numerous other challenges. The most important is that it is not compatible with the current mode in which the dual-polarized WSR-88D operates (i.e., SHV); hence, switching to the AHV mode would require significant changes in the existing algorithms. Even more, obtaining the dual-polarization variables with required quality, while maintaining unambiguous range of ~300 km, may be more challenging. On the other hand, if the SHV is used for the polarimetric PAR (PPAR) the current algorithms can be seamlessly transferred to the new hardware. Further, advantages of SHV mode are: 1) produces estimates with significant lower errors for the same scan rates, 2) the differential phase is measured within a 360° interval, 3) the correlation coefficient $|\rho_{hv}(0)|$ can be measured directly (i.e., no need to assume a correlation model), 4) there are no compromises in the performance of the ground clutter

Corresponding author address: Igor R. Ivić, CIMMS/NSSL, 120 David L. Boren Blvd., Norman, OK 73072; email: Igor.Ivic@noaa.gov

filter. This compels us to search for alternate ways to improve cross-polar isolation that would suit the PPAR design and enable the SHV mode with satisfactory Z_{DR} bias.

Orthogonal coding in the SHV mode to enable cross-polar measurements was proposed by Giuli et al. (1993) and after that by Stagliano et al. (2006) without specifying the code details (see also Stagliano et al. 2009) in the latter case. Chandrasekhar and Bharadwaj (2009) proposed to reduce the cross-polar isolation by implementing phase changes on transmission from pulse to pulse using Welsh-Hadamard codes. The scheme operates by shifting the spectrum of one of the signals (H or V) by half the Nyquist interval so that after it couples with the other signal it can be removed by filtering. Also, a scheme is proposed by Zrnić et al. (2013) whereby modulations similar to Sachidananda and Zrnić (1986) are used to achieve the same goal. Both schemes can be successful in suppressing contaminants even without the use of filtering (at the expense of a moderate increase in variance). Clearly, both schemes require that the Nyquist interval be large enough so that the spectra of two signals do not overlap (for the most part) and filtering can succeed in removing unwanted cross-polar signals. However, in the current implementation on the WSR-88D, the polarimetric variables at the lowest two (sometimes three) elevation angles are obtained in the SHV mode using long pulse repetition time (over 3 ms) so that range ambiguities do not occur. Such long repetition times result in small Nyquist velocities which prevent successful filtering of the contaminant signal, which may render bias removal less effective in such cases. Additionally, it is likely that the application of phase codes on a pulse to pulse basis (interpulse coding) may require minimum number of pulses per dwell to be effective. Because it is likely that the PPAR will be designed for weather observation as well as aircraft detection and tracking (Weadon et al. 2009) it will have to share resources between these two roles. This will impose stringent requirements on the dwell times allowed for weathers scans. Hence, the number of pulses collected per dwell may not be sufficient for effective bias removal using the interpulse coding; rather, sophisticated schemes may be developed that will maintain the existing quality of weather products but use much shorter dwell times by decreasing the number of pulses per dwell.

2. THEORETICAL MODEL

The backscattering properties of a single hydrometeor can be described by its backscattering matrix **S** which relates the backscattered electric filed $\mathbf{E}_b$ at the antenna to the incident one $\mathbf{E}_i$ (Doviak and Zrnić 2001)

$$\mathbf{E}_b \sim \begin{bmatrix} s_{hh} & s_{hv} \\ s_{vh} & s_{vv} \end{bmatrix} \mathbf{E}_i \qquad (1)$$

where *h* denotes the horizontal (H) and *v* the vertical (V) polarization. The presence of distributed scatterers (e.g., precipitation) between the resolution volume and radar may alter the transmitted electric wave as it propagates through it. This is known as propagation effect and is usually quantified by the transmission matrix **T**. Assuming there is no depolarization on propagation the differential phase shift (Φ_{DP}) is the dominant effect and for linear orthogonal polarization **T** is

$$\mathbf{T} = \begin{bmatrix} \exp\left(-j\Phi_{DP}/2\right) & 0 \\ 0 & 1 \end{bmatrix}. \qquad (2)$$

Additionally, the practical antennas and the associated microwave circuitry introduce change in polarization which are described by the matrix **F**. These are analyzed by Zrnić et al. (2010) who give this matrix as

$$\mathbf{F} = \begin{bmatrix} F_{hh} & F_{hv} \\ F_{vh} & F_{vv} \end{bmatrix}, \qquad (3)$$

where it is assumed that the pattern functions F_{ij} (where *i,j* designate polarization *h* or *v*) and β (differential phase between the H and V on transmission) are constant. The one way pattern functions F_{ij} (where *i,j* designate polarization *h* or *v*) are not normalized but contain the peak power gain g_{ij} so that

$$F_{ij}(\theta,\phi) = \sqrt{g_{ij}} f_{ij}(\theta,\phi) \qquad (4)$$

where $f_{ij}(\theta, \phi)$ is the normalized antenna pattern. F_{hv} is proportional to the H radiated electric field if the V channel is excited, and vice versa for F_{vh}. F_{hh} and F_{vv} are assumed to be real functions (i.e., have zero reference phase), but F_{hv}, F_{vh} are complex (i.e., F_{hv} and F_{vh} have phases γ_{hv} and γ_{vh} relative to the phase of copolar H). Constants of proportionality that would make this equation dimensionally correct, and the arguments of F_{ij} and s_{ij}, are omitted to shorten the notation; these omissions have no effect on the results.

Let us denote the samples of a received phase coded signals from the sequences of simultaneously transmitted pulses (spaced in time by T_s), in the horizontal (H) and the vertical (V) channels, as $V_h^c(m)$ and $V_v^c(m)$ where *m* is the sequence index. The phase codes $\alpha_h(m)$ and $\alpha_v(m)$ are imposed on the pulses generated at the radar transmitter system (Klystron, TWT, or solid state). As these pulses propagate through media they illuminate scatterers and a portion of the energy is returned towards the radar. Returned energy, at time *t* (measured from the start of the *m*-th

transmission), from a volume in the direction (θ, ϕ) located at distance r from the radar, creates voltage increments $\delta V_h(t, r)$ and $\delta V_v(t, r)$ at the antenna output. Hence, $\delta V_h(t,r)$ and $\delta V_v(t,r)$ can be viewed as returns at time t from a vanishingly thin spherical shell located in the spherical direction determined by angles θ, ϕ, at distance r from the radar, weighted by the transmitted pulse and the antenna radiation pattern $f(\theta, \phi)$. We carry on further analysis assuming the following: 1) radar returns are produced by depolarizing scatterers (but mean canting angles of scatterers on propagation are zero) so the off-diagonal terms of the backscattering matrix are not zero, 2) there is a differential phase β between the transmitted H and V copolar radiation fields, and 3) differential attenuation along the path of propagation can, for most observations at 10-cm wavelengths, be neglected, but the differential phase (Φ_{DP}) cannot be ignored. Next, we use the extended notation from Zrnić et al. (2010) to express the incremental voltages in the H and V channels generated by the scatterers.

Next, using the notation presented so far we express coupling due to antenna cross polar pattern and the scattering media. The results are applicable to other couplings as well; hence what follows is very general. Thus, the horizontally and vertically polarized signals received from a hydrometeor at a time mT_s are (Zrnić et al. (2010, Eq.3)

$$\begin{bmatrix} \delta V_h(t,r) \\ \delta V_v(t,r) \end{bmatrix} \equiv \vec{V} = \mathbf{F}^t \mathbf{S} \mathbf{F} \vec{E}_i = \begin{bmatrix} F_{hh} & F_{vh} \\ F_{hv} & F_{vv} \end{bmatrix} \begin{bmatrix} s_{hh} e^{-j\Phi_{DP}} & s_{hv} e^{-j\frac{\Phi_{DP}}{2}} \\ s_{vh} e^{-j\frac{\Phi_{DP}}{2}} & s_{vv} \end{bmatrix} \times \begin{bmatrix} F_{hh} & F_{hv} \\ F_{vh} & F_{vv} \end{bmatrix} \begin{bmatrix} e^{j\alpha_h} \\ e^{j(\beta+\alpha_h)} \end{bmatrix} \quad (5)$$

where it is assumed that the pattern functions F_{ij} (where i,j designate polarization h or v) and β (differential phase between the H and V on transmission) are constant and all other variables are functions of m. In the interest of compactness, we merge the Φ_{DP} with the scatterer's backscatter differential phase in following considerations. To describe the effects of depolarization by the scattering media we have the following defined

$$LDR = \frac{\left\langle |s_{hv}(m)|^2 \right\rangle}{\left\langle |s_{hh}(m)|^2 \right\rangle}$$
$$\rho_{xh} e^{j\frac{\Phi_{DP}}{2}} = \frac{\left\langle s_{hh}^*(m) s_{hv}(m) \right\rangle}{\sqrt{|s_{hh}(m)|^2 |s_{hv}(m)|^2}} \quad (6)$$
$$\rho_{xv} e^{-j\frac{\Phi_{DP}}{2}} = \frac{\left\langle s_{vv}^*(m) s_{hv}(m) \right\rangle}{\sqrt{|s_{vv}(m)|^2 |s_{hv}(m)|^2}}$$

where LDR is the linear depolarization ratio (Doviak and Zrnić 2006), and ρ_{xh} and ρ_{xv} are co-cross-polar correlation coefficients (Ryzhkov 2001). The effects of the phase difference due to differential phase shifts within the receiver are neglected as they have no bearing on the results reported herein. The voltage increments δV_h and δV_v consist of contributions by scatterers from the direction (θ, ϕ). In azimuth, the function F (Doviak and Zrnić 2006; eq.8.43a) weighting the contributions of each scatterer has a random phase $\psi(\theta, \phi)$ uncorrelated from one solid angle $d\Omega$ to the next, and is proportional to the intensity and phase of the radiation pattern at angles θ, ϕ. The received voltages are

$$\begin{aligned} V_h^c(m) \sim \int_\Omega \Big\{ \Big[& F_{hh}^2 s_{hh}(m) + F_{vh}^2 s_{vv}(m) + \\ & F_{hh} F_{vh} s_{vh}(m) + F_{hh} F_{vh} s_{hv}(m) \Big] e^{j\alpha_h(m)} + \\ \Big[& F_{hh} F_{hv} s_{hh}(m) + F_{vv} F_{vh} s_{vv}(m) + \\ & F_{hh} F_{vv} s_{hv}(m) + F_{hv} F_{vh} s_{vh}(m) \Big] e^{j(\beta+\alpha_v(m))} \Big\} e^{j\psi_h(\theta,\varphi)} d\Omega \\ V_v^c(m) \sim \int_\Omega \Big\{ \Big[& F_{hv}^2 s_{hh}(m) + F_{vv}^2 s_{vv}(m) + \\ & F_{vv} F_{hv} s_{vh}(m) + F_{vv} F_{hv} s_{hv}(m) \Big] e^{j(\beta+\alpha_v(m))} \\ \Big[& F_{hh} F_{hv} s_{hh}(m) + F_{vv} F_{vh} s_{vv}(m) + \\ & F_{hh} F_{vv} s_{vh}(m) + F_{hv} F_{vh} s_{hv}(m) \Big] e^{j\alpha_h(m)} \Big\} e^{j\psi_v(\theta,\varphi)} d\Omega. \end{aligned} \quad (7)$$

After decoding and assuming reciprocity (i.e., $s_{hv} = s_{vh}$) we get

$$
\begin{aligned}
V_h(m) \sim & \int_{\Omega} \{ F_{hh}^2 s_{hh}(m) + F_{vh}^2 s_{vv}(m) + \\
& 2F_{hh}F_{vh}s_{hv}(m) + \\
& \left[F_{hh}F_{hv}s_{hh}(m) + F_{vv}F_{vh}s_{vv}(m) + \right. \\
& \left. \left(F_{hh}F_{vv} + F_{hv}F_{vh}\right)s_{hv}(m) \right] e^{j(\beta+\alpha_v(m)-\alpha_h(m))} \} e^{j\psi_h(\theta,\varphi)} d\Omega \\
V_v(m) \sim & \int_{\Omega} \{ \left[F_{hv}^2 s_{hh}(m) + F_{vv}^2 s_{vv}(m) + \right. \\
& \left. 2F_{vv}F_{hv}s_{hv}(m) \right] e^{j\beta} + \\
& \left[F_{hh}F_{hv}s_{hh}(m) + F_{vv}F_{vh}s_{vv}(m) + \right. \\
& \left. \left(F_{hh}F_{vv} + F_{hv}F_{vh}\right)s_{hv}(m) \right] e^{j(\alpha_h(m)-\alpha_v(m))} \} e^{j\psi_v(\theta,\varphi)} d\Omega
\end{aligned}
\tag{8}
$$

Now let us consider power estimates computed as

$$
\begin{aligned}
\left|V_h(m)\right|^2 &= \int_{\Omega} \left(F_{hh}^4 \left|s_{hh}(m)\right|^2 + \delta P_h(m) \right) d\Omega \\
\left|V_v(m)\right|^2 &= \int_{\Omega} \left(F_{vv}^4 \left|s_{vv}(m)\right|^2 + \delta P_v(m) \right) d\Omega
\end{aligned}
\tag{9}
$$

where $\delta P_h(m)$ and $\delta P_v(m)$ are bias inducing terms in the H and V power estimates). These are derived in APPENDIX A as

$$
\begin{aligned}
\delta P_h(m) &\approx \int_{\Omega} \left[A_h(m) + \right. \\
& \left. 2\mathrm{Re}\left\{ B_h(m) e^{j(\beta+\alpha_v(m)-\alpha_h(m))} \right\} \right] d\Omega \\
\delta P_v(m) &\approx \int_{\Omega} \left[A_v(m) + \right. \\
& \left. 2\mathrm{Re}\left\{ B_v(m) e^{-j(\beta+\alpha_v(m)-\alpha_h(m))} \right\} \right] d\Omega
\end{aligned}
\tag{10}
$$

where $A_c(m)$ and $B_c(m)$ (c is h or v) are defined in APPENDIX A. Note that the phase codes bear no impact on the $A_h(m)$ and $A_v(m)$ in (10). These, however, are not the main contributors to the bias because the only terms where F_{hh} and F_{vv} appear on the third order are scaled by the linear depolarization ratio (*LDR*), imposed by the depolarized scatterers, which takes upon values of -25 dB or smaller (Ryzhkov 2001).

Next, we consider the expected value of the overall power sum as

$$
\left\langle \hat{P}_c \right\rangle = \frac{1}{M} \sum_{m=0}^{M-1} \left\langle \hat{P}_c(m) \right\rangle \tag{11}
$$

where c is h or v. Derivation of the result when two consecutive terms in (11) are summed is given in APPENDIX B. It shows that if

$$
\begin{aligned}
& \cos\left(\alpha_h(m) - \alpha_v(m)\right) = \\
& -\cos\left(\alpha_h(m+1) - \alpha_v(m+1)\right) \\
& \sin\left(\alpha_h(m) - \alpha_v(m)\right) = \\
& -\sin\left(\alpha_h(m+1) - \alpha_v(m+1)\right)
\end{aligned}
\tag{12}
$$

the bias terms that are affected by the phase codes, in both H and V, cancel each other. We then have

$$
\begin{aligned}
\left\langle \hat{P}_h(m) \right\rangle + \left\langle \hat{P}_h(m+1) \right\rangle &\approx 2 \int_{\Omega} \left[F_{hh}^4 \left\langle \left|s_{hh}(m)\right|^2 \right\rangle + \right. \\
& \left. \left\langle A_h(m) \right\rangle \right] d\Omega \\
\left\langle \hat{P}_v(m) \right\rangle + \left\langle \hat{P}_v(m+1) \right\rangle &\approx 2 \int_{\Omega} \left[F_{vv}^4 \left\langle \left|s_{vv}(m)\right|^2 \right\rangle + \right. \\
& \left. \left\langle A_v(m) \right\rangle \right] d\Omega
\end{aligned}
\tag{13}
$$

Simple solution is to have

$$
\alpha_v(m) - \alpha_h(m) = \alpha + m\pi \tag{14}
$$

where α can be any angle. These conditions are met if the phases on transmission are

$$
\begin{aligned}
\alpha_h(m) &= \varphi \\
\alpha_v(m) &= \varphi + \alpha + m\pi \\
\alpha_h(m+1) &= \eta \\
\alpha_v(m+1) &= \eta + \alpha + (m+1)\pi
\end{aligned}
\tag{15}
$$

Where φ and η can take upon any values between -π and π. Hence, it is possible to impose the varying phase on the transmitted pulses without upsetting the function of the phase codes. Clearly, if M is even all bias terms cancel but if M is odd one still remains. To account for the latter case we can set the following requirement

$$
\begin{aligned}
& \left\langle \delta P_h(0) \right\rangle + \left\langle \delta P_h(1) \right\rangle + \left\langle \delta P_h(2) \right\rangle \approx \\
& 2 \int_{\Omega} \left[\mathrm{Re}\left\{ \left\langle B_h(m) \right\rangle \left(e^{j(\beta+\alpha_v(0)-\alpha_h(0))} + \right. \right. \right. \\
& \left. \left. \left. e^{j(\beta+\alpha_v(1)-\alpha_h(1))} + e^{j(\beta+\alpha_v(2)-\alpha_h(2))} \right) \right\} d\Omega = 0
\end{aligned}
\tag{16}
$$

We can achieve this by setting the phase of the first three transmissions so that

$$
\begin{aligned}
& \cos\left(\alpha_v(0) - \alpha_h(0)\right) + \cos\left(\alpha_v(1) - \alpha_h(1)\right) + \\
& \cos\left(\alpha_v(2) - \alpha_h(2)\right) = 0 \\
& \sin\left(\alpha_v(0) - \alpha_h(0)\right) + \sin\left(\alpha_v(1) - \alpha_h(1)\right) + \\
& \sin\left(\alpha_v(2) - \alpha_h(2)\right) = 0
\end{aligned}
\tag{17}
$$

One possible solution is

$$\begin{aligned}\alpha_v(0)-\alpha_h(0)&=\alpha\\ \alpha_v(1)-\alpha_h(1)&=\alpha+\arccos(-0.5)\\ \alpha_v(2)-\alpha_h(2)&=\alpha-\arccos(-0.5)\end{aligned} \tag{18}$$

Examination of the cross-correlation computation

$$\hat{R}_{hv}(0)=\frac{1}{M}\sum_{m=0}^{M-1}V_v^*(m)V_v(m) \tag{19}$$

is given in APPENDIX C. It shows that while phase codes are effective in removing cross-polar contaminants produced by the radar hardware, the significant bias terms caused by depolarizing media still remain.

3. ESTIMATION QUALITY ASSESSMENT

For simplicity we assume the uniform beam filling, hence $s_{cc}(m)$ (where c is either h or v) is not function of Ω. We also assume the shapes of the copolar and cross-polar patterns to differ only by phase (i.e., F_{hh} = F_{vv} = $|F_{hv}|$ = $|F_{vh}|$). Such assumption certainly holds for coupling through radar hardware and in the case of coupling through radiation patterns it assumes the worst possible case. This is because the cross-polar patterns can have shapes different than the copolar ones (e.g., four-lobed pattern given in Zrnić et al. 2010), in which case the cross-polar coupling is much less detrimental than in the assumed case. Next, we apply normalization so that

$$\begin{aligned}&\int_\Omega\left|f_{ij}(\theta,\phi)\right|^4 d\Omega=\int_\Omega\left|f(\theta,\phi)\right|^4 d\Omega=1\\ &g_{hh}=g_{vv}=g\end{aligned}. \tag{20}$$

Given the assumption that all the radiation patterns are the same in shape and that cross-polar isolation is the same in H and V we define the cross-polar suppression (*CPS*) on transmission as

$$CPS=\frac{\left|F_{hv}(\theta)\right|^2}{F_{hh}^2(\theta)}=\frac{g_{hv}}{g}=\frac{\left|F_{vh}(\theta)\right|^2}{F_{vv}^2(\theta)}=\frac{g_{vh}}{g} \tag{21}$$

which is the ratio similar to the ratios presented in Figure 5. of Zrnić et al. 2010. Given these assumptions we can represent

$$\begin{aligned}F_{vh}&=\sqrt{g\bullet CPS}\bullet f(\theta,\phi)e^{j\gamma_{vh}}\\ F_{hv}&=\sqrt{g\bullet CPS}\bullet f(\theta,\phi)e^{j\gamma_{hv}}\end{aligned} \tag{22}$$

which allows us to integrate along Ω as

$$\begin{aligned}\left|V_h(m)\right|^2&\approx\int_\Omega\left[F_{hh}^4\left|s_{hh}(m)\right|^2+\delta P_h(m)\right]d\Omega\\ &\approx g^2\left|s_{hh}(m)\right|^2+\delta P_h'(m)\\ \left|V_v(m)\right|^2&\approx\int_\Omega\left[F_{hh}^4\left|s_{vv}(m)\right|^2+\delta P_v(m)\right]d\Omega\\ &\approx g^2\left|s_{vv}(m)\right|^2+\delta P_v'(m)\end{aligned} \tag{23}$$

where $\delta P'_h(m)$ and $\delta P'_v(m)$ are given in APPENDIX A. This approach provides for investigating the effects of cross-coupling where we generate $s_{hh}(m)$ and $s_{vv}(m)$ using Monte Carlo simulations (Zrnić 1975, Torres 2001). Explanation of how $s_{hv}(m)$ is simulated is given in APPENDIX D. Note that because we are investigating the properties of differential reflectivity which is the ratio of powers from H and V we can set g to one for the purposes of simulation.

Let us examine the differential reflectivity. It is computed as

$$\hat{Z}_{DR}=10\log_{10}\left(\frac{\hat{S}_h^{NC}+\delta\hat{P}_h}{\hat{S}_v^{NC}+\delta\hat{P}_v}\right), \tag{24}$$

where superscript *NC* denotes the estimates unbiased by the cross-coupling (i.e., F_{hv} = F_{vh} = 0) and

$$\begin{aligned}\hat{S}_h^{NC}&=\frac{1}{M}\sum_{m=0}^{M-1}\left|s_{hh}(m)\right|^2-N_h\\ \hat{S}_v^{NC}&=\frac{1}{M}\sum_{m=0}^{M-1}\left|s_{vv}(m)\right|^2-N_v\\ \delta\hat{P}_h&=\frac{1}{M}\sum_{m=0}^{M-1}\delta\hat{P}_h'(m)\\ \delta\hat{P}_v&=\frac{1}{M}\sum_{m=0}^{M-1}\delta\hat{P}_v'(m)\end{aligned} \tag{25}$$

where N_h and N_v are noise powers in H and V channels. After developing into Taylor series of the first order and taking mathematical expectations it becomes

$$\left\langle\hat{Z}_{DR}\right\rangle\approx\left\langle\hat{Z}_{DR}^{NC}\right\rangle+\frac{10}{\ln(10)}\frac{\left\langle\delta\hat{P}_h\right\rangle}{\left\langle\hat{S}_h^{NC}\right\rangle}-\frac{10}{\ln(10)}\frac{\left\langle\delta\hat{P}_v\right\rangle}{\left\langle\hat{S}_v^{NC}\right\rangle} \tag{26}$$

where the first term stands for the differential reflectivity when no cross-coupling is present and the rest of the terms contribute to the bias. Using expressions from APPENDIX A we get for the expected bias when no phase coding is applied and the terms $A'_h(m)$ and $A'_v(m)$ are ignored

$$\left\langle BIAS\left(\hat{Z}_{DR}\right)\right\rangle \approx \frac{20g^2}{\ln(10)}\Big[2\sqrt{CPS}LDR\left(\cos\left(\beta-\gamma_{vh}\right)-Z_{dr}\cos\left(\beta+\gamma_{hv}\right)\right)+\sqrt{LDR}\cos\left(\beta+\frac{\Phi_{DP}}{2}\right)\left(\rho_{xh}-\rho_{xv}\sqrt{Z_{dr}}\right)+\sqrt{CPS}\left(\cos\left(\gamma_{hv}+\beta\right)-\cos\left(\gamma_{vh}-\beta\right)\right)+\sqrt{CPS}\left|\rho_{hv}(0)\right|\left(\frac{\cos\left(\gamma_{vh}+\beta+\Phi_{DP}\right)}{\sqrt{Z_{dr}}}-\sqrt{Z_{dr}}\cos\left(\gamma_{hv}-\beta-\Phi_{DP}\right)\right)\Big] \quad (27)$$

If we take that there is no depolarization in the media (i.e., *LDR* = 0) the formula becomes equivalent to eq. 13 in Zrnić et al. 2010. As pointed out in Zrnić et al. (2010) the bias in Z_{DR} is dependent on the values of β, γ_{hv}, and γ_{vh}. The maximum positive bias occurs if

$$\begin{aligned}\gamma_{hv}+\beta&=0\\ \gamma_{vh}-\beta&=\pi\\ \gamma_{vh}+\beta+\Phi_{DP}&=0\\ \gamma_{hv}-\beta-\Phi_{DP}&=\pi\end{aligned} \quad . \quad (28)$$

In general, these conditions are met if

$$\begin{aligned}\gamma_{hv}&=-\beta\\ \gamma_{vh}&=\pi+\beta\\ \beta&=-\frac{\pi+\Phi_{DP}}{2}\end{aligned} \quad . \quad (29)$$

If cross-polar patterns have four axis symmetric principal lobes of equal magnitude then $\gamma_{hv} = \gamma_{vh} = \gamma$ (Zrnić et al. 2010) and the maximum positive bias occurs for

$$\begin{aligned}\gamma&=\frac{\pi}{2}\\ \beta&=-\frac{\pi}{2}\\ \Phi_{DP}&=0\end{aligned} \quad . \quad (30)$$

which is the same result as obtained by Zrnić et al. 2010. Bias was also examined using simulations. Using simulations Z_{DR} biases were examined for all combinations of β and γ when depolarization in the scattering media is present and when it is not (in the latter case *LDR* = -Inf dB). The bias is computed as

$$BIAS\left(\hat{Z}_{DR}\right)=\frac{1}{K}\sum_{k=0}^{K-1}\left(10\log_{10}\left(\frac{\frac{1}{M}\sum_{m=0}^{M-1}\left|S_{hh}(m,k)\right|^2}{\frac{1}{M}\sum_{m=0}^{M-1}\left|S_{vv}(m,k)\right|^2}\right)-10\log_{10}\left(\frac{\frac{1}{M}\sum_{m=0}^{M-1}\left|V_h(m,k)\right|^2}{\frac{1}{M}\sum_{m=0}^{M-1}\left|V_v(m,k)\right|^2}\right)\right) \quad (31)$$

where *K* is the number of simulation runs, and *k* designator is used to denote the simulated sample number. Note that the bias computed in (31) is the additional bias added to the inherent Z_{DR} estimator bias. The results for the non-phased coded data when *CPS* is 40 dB and $\gamma_{hv} = \gamma_{vh} = \gamma$ are presented in Figure 1. Cross Polar suppression of 40 dB is achievable in radars with parabolic dish antennas (e.g., WSR-88D, Zrnić et al. 2010). Figure 1 (a) shows the bias as function of Z_{DR} for the combination of phases in (30) when depolarization by scatterers is presents and when it is not. It demonstrates that, for the assumed conditions, differential reflectivity bias can exceed the preferable value of 0.1 dB in the worst case. It is interesting to note that the presence of depolarization by the media reduces the bias somewhat in this particular case. This effect is produced by the depolarization terms in (27) whose overall bias is negative for the given conditions. In general though, the overall bias increases significantly in the presence of depolarization by scatterers as can be seen from Figure 1 (d). Moreover, Figure 1 (b) shows that the bias exceeds 0.1 dB for most of the Φ_{DP} values if $\gamma = \pi/2$ and $\beta = -\pi/2$.

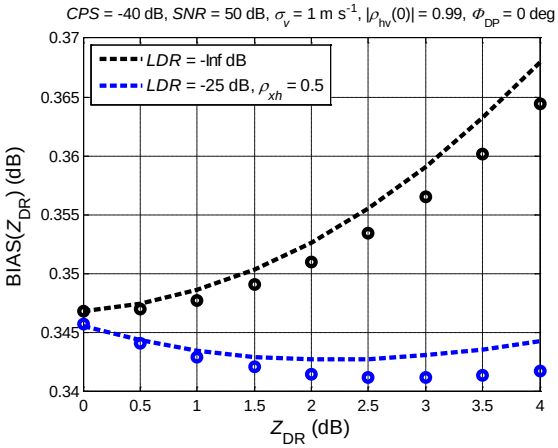

(a)

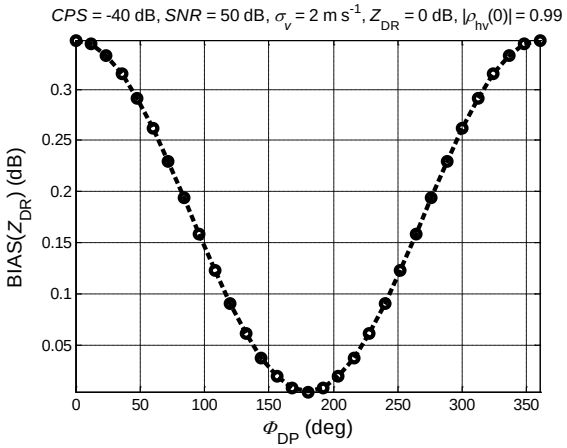

(b)

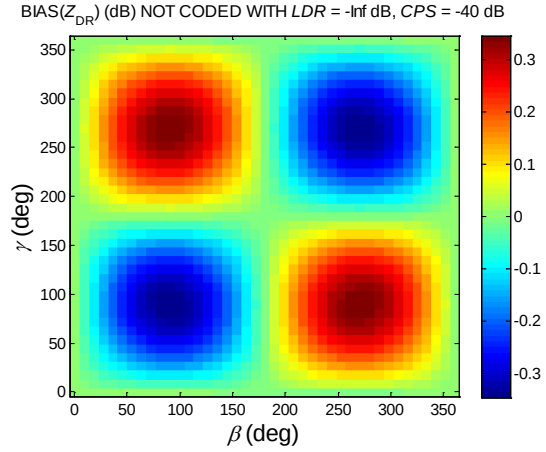

(c)

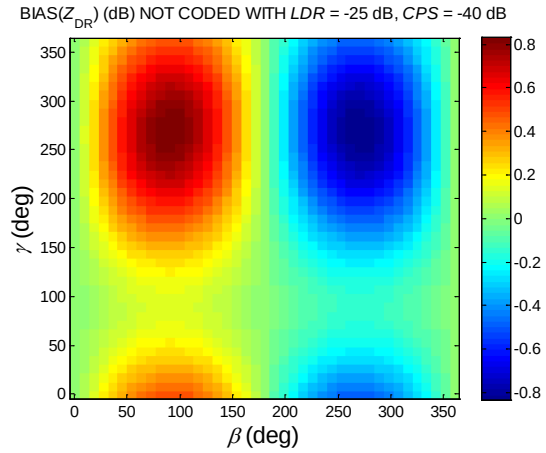

(d)

Figure 1. Differential reflectivity bias for simulated data with M = 16, *SNR* = 50 dB, for *CPS* of 40 dB. Biases are shown for a range (a) of Z_{DR} values (results of perturbation are given in circles), (b) of Φ_{DP} values (results of perturbation are given in circles), (c) of γ and β when Φ_{DP} = 0º and LDR = 0, and (d) of γ and β when Φ_{DP} = 0º and LDR = -25 dB.

Next, we examine the effectiveness of the phase codes. Since the codes are designed to cancel the bias terms caused by the B_h(m) and B_v(m) the bias is primarily induced by the A_h(m) and A_v(m) terms; hence, the bias is not dependent on β. For the case when no depolarization in the media is present the bias can be expressed as

$$\begin{aligned}\left\langle BIAS_C\left(\hat{Z}_{DR}\right)\right\rangle \approx \frac{20g^2}{\ln(10)}\Bigg[&CPS\left(1+\frac{1}{Z_{dr}}\right)- \\ &CPS\left(1+Z_{dr}\right)+ \\ &2CPS\left|\rho_{hv}(0)\right|\Bigg(\frac{\cos\left(\gamma_{vh}-\gamma_{hv}+\Phi_{DP}\right)}{\sqrt{Z_{dr}}}- \\ &\sqrt{Z_{dr}}\cos\left(\gamma_{hv}-\gamma_{vh}-\Phi_{DP}\right)+ \\ &\frac{\cos\left(2\gamma_{vh}+\Phi_{DP}\right)}{\sqrt{Z_{dr}}}-\sqrt{Z_{dr}}\cos\left(2\gamma_{hv}-\Phi_{DP}\right)\Bigg)\Bigg]\end{aligned} \tag{32}$$

From the expression (32) it can be inferred that the largest positive bias occurs when

$$\begin{aligned}\gamma_{vh}-\gamma_{hv}+\Phi_{DP}&=0\\ \gamma_{hv}-\gamma_{vh}-\Phi_{DP}&=\pi\\ 2\gamma_{vh}+\Phi_{DP}&=0\\ 2\gamma_{hv}-\Phi_{DP}&=\pi\end{aligned} \tag{33}$$

This set of equations is over determined so such case can never take place. However, the last two terms in (32) add up constructively if

$$\begin{aligned}\gamma_{hv}&=\frac{\pi-\Phi_{DP}}{2}\\ \gamma_{vh}&=-\frac{\Phi_{DP}}{2}\end{aligned} \tag{34}$$

Thus, in Figure 2 (a) and (b) bias is shown for a range of differential reflectivity values for *CPS* of 20 and 25 dB; the first suppression is easily achievable in phased arrays whereas latter requires use of sophisticated designs. It can be observed that points when the largest bias occurs is for Φ_{DP} = 0º. When *CPS* is 20 dB, the 0.1 dB bias requirement is not met for a large range of Φ_{DP} values. On the contrary, when *CPS* is 25 dB the bias requirement is satisfied along the entire Φ_{DP} range when *LDR* is zero. This implies that the cross-polar suppression of at least -25 dB is preferable. Consequently, the bias is given for a range of Z_{DR} values in Figure 2 (c) for *CPS* of 25 dB.

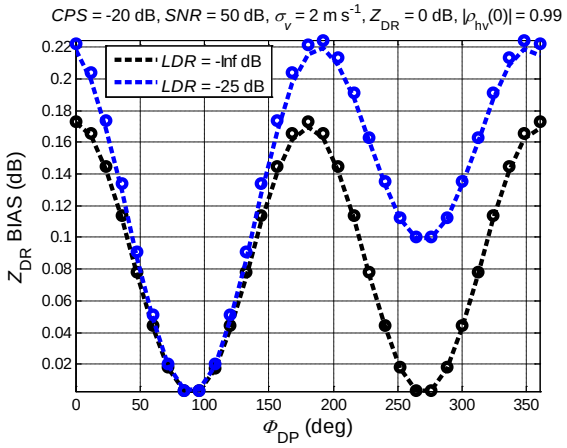

(a)

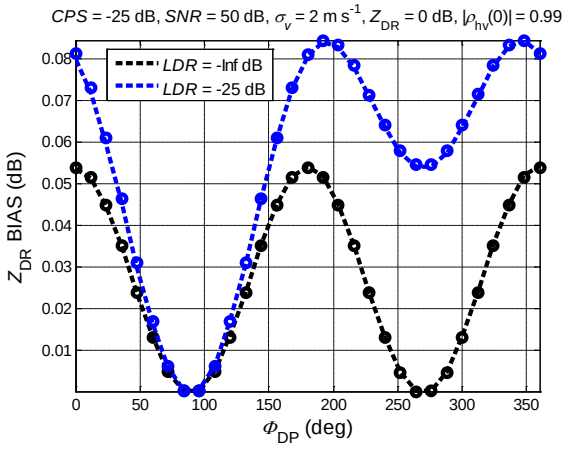

(b)

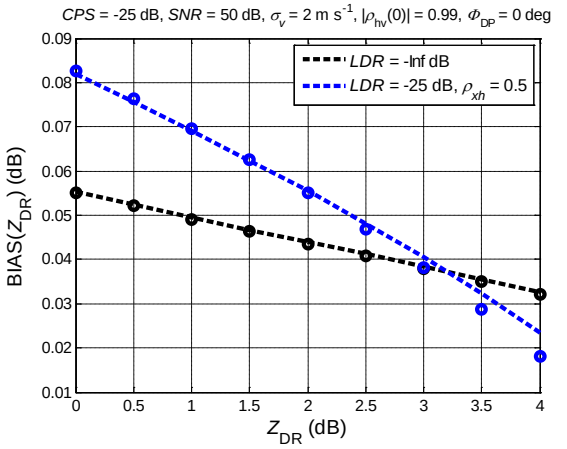

(c)

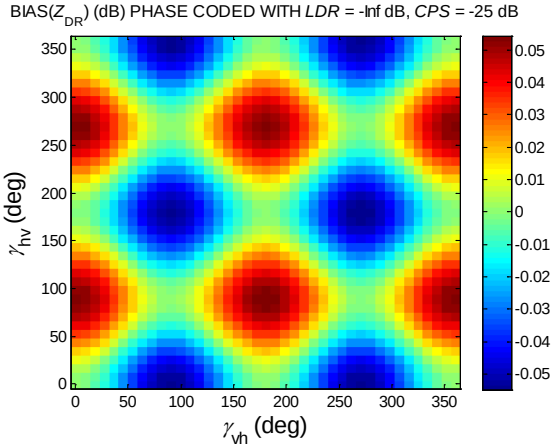

(d)

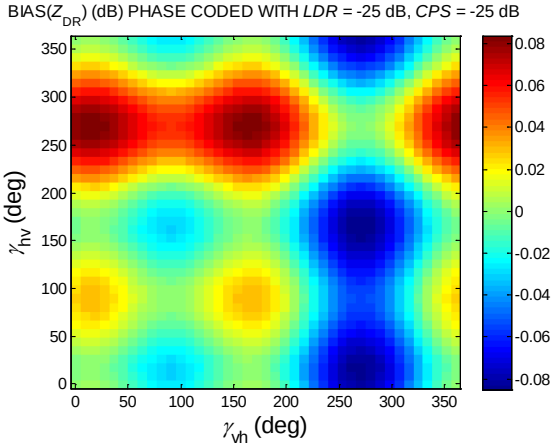

(e)

Figure 2. Differential reflectivity bias for phase coded simulated data with M = 16, SNR = 50 dB, Z_{DR} = 0 dB, Φ_{DP} = 0° for different values of LDR and CPS.

To examine how bias changes with number of samples it is computed for range of M values and shown in Figure 3. Figure 3 (a) shows bias obtained simulations and theoretical analysis when only codes in (15) are used. As expected, bias significantly increases for odd M, but generally bias differences between even and odd number of samples declines as M increases. Figure 3 (b) is obtained setting phases of the first three samples as in (18). This equalizes the performance of phase codes for even and odd number of samples.

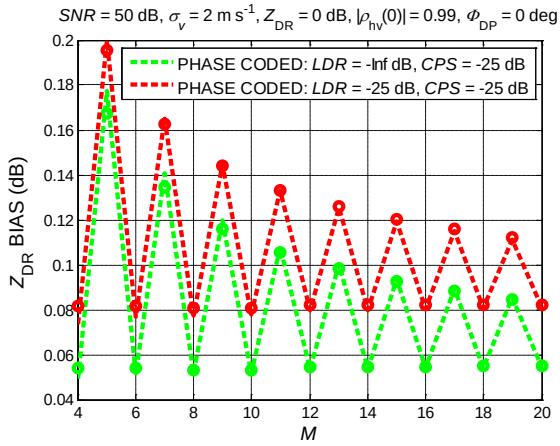

(a)

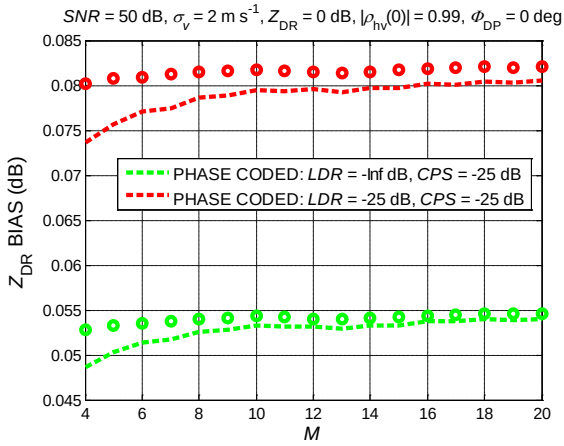

(b)

Figure 3. Z_{DR} bias for different values of *M*. Dashed lines are produced using simulations and circles are obtained using perturbation analysis. (a) Only phase codes for even number of samples are applied. (b) Phase codes for both even and odd number samples are applied.

Next, we examine the standard deviations of differential reflectivity. Assessment of variance using perturbation analysis is given in APPENDIX E. The expression for variance assuming no phase coding and *LDR* of zero is

$$\begin{aligned} &Var\left(\hat{Z}_{DR}\right) \approx Var\left(\hat{Z}_{DR}^{NC}\right) + \\ &g^2 \frac{200}{\ln^2(10)}\left[CPS\left(2\frac{1-\left|\rho_{hv}(0)\right|^2}{M_l} + \right.\right. \\ &\left.\left.\frac{\left|\rho_{hv}(0)\right|^2 - 1}{M_l}\left(Z_{dr} + \frac{1}{Z_{dr}}\right)\right) + \right. \\ &\left. 2\sqrt{CPS}\frac{1-\left|\rho_{hv}(0)\right|^2}{M_l} \times \right. \\ &\left.\left(\cos\left(\gamma_{hv} + \beta\right) + \cos\left(\gamma_{vh} - \beta\right)\right)\right] \end{aligned} \tag{35}$$

From (35) it is seen that the maximal additional variance, induced by the cross-polar contaminants, is when

$$\begin{aligned} \gamma_{hv} &= -\beta \\ \gamma_{vh} &= \beta \end{aligned} \tag{36}$$

Additionally, variances are also computed using simulations as

$$\begin{aligned} Var\left(\hat{Z}_{DR}\right) = \frac{100}{K-1}\sum_{k=0}^{K-1}\left[\log_{10}\left(\frac{\frac{1}{M}\sum_{m=0}^{M-1}\left|V_{hh}(m,k)\right|^2}{\frac{1}{M}\sum_{m=0}^{M-1}\left|V_{vv}(m,k)\right|^2}\right) - \right. \\ \left.\frac{1}{K}\sum_{l=0}^{K-1}\log_{10}\left(\frac{\frac{1}{M}\sum_{m=0}^{M-1}\left|V_{hh}(m,l)\right|^2}{\frac{1}{M}\sum_{m=0}^{M-1}\left|V_{vv}(m,l)\right|^2}\right)\right]^2 \end{aligned} \tag{37}$$

for various values of *LDR* and *CPS*. Standard deviations are obtained from those as

$$SD\left(\hat{Z}_{DR}\right) = \sqrt{Var\left(\hat{Z}_{DR}\right)}. \tag{38}$$

Results of the standard deviations estimation are shown in Figure 4. Figure 4 (a) presents results obtained using simulations and perturbations analysis (results of the latter are shown in circles); standard deviation of Z^{NC}_{DR} is computed using expression from Melnikov and (35) is used to add variance induced by the cross-coupling contaminants. These demonstrate that even if CPS = 25 dB the cross-coupling terms add only about 10% to the overall standard deviation. Moreover, the phase coding reduces the standard deviation and makes it almost equal to the case when no cross-coupling terms are present. This can be attributed to the fact that the phase codes are designed to minimize the effect of the terms that contribute most to the Z_{DR} bias and this function extends to variance as well; hence, the terms multiplied by

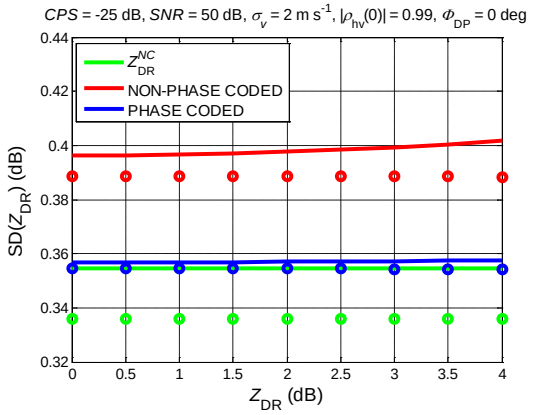

(a)

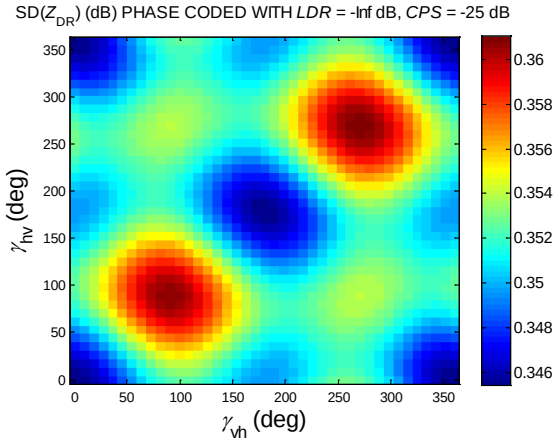

(b)

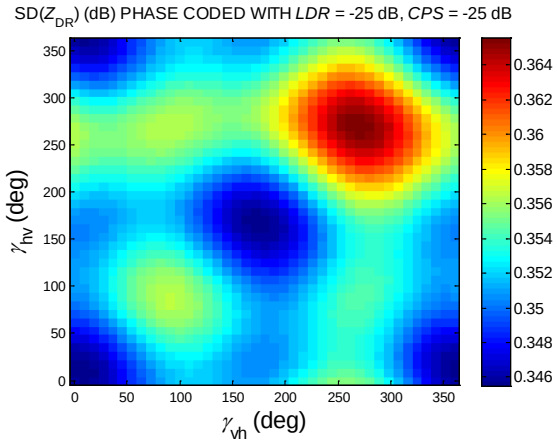

(c)

Figure 4. Standard deviations for data with M = 16, SNR = 50 dB, and CPS = 25 dB. (a) The phase coded data compared to the non-phase coded and non-contaminated data (perturbation results are shown in circles). (b) and (c) Simulations for a range of γ_{hv} and γ_{vh} values and Z_{DR} = 0 dB, Φ_{DP} = 0°.

Next, we examine biases on a radial of real time-series collected by the WSR-88D research radar in Norman, OK. The SNR profile is shown in Figure 5 (a) and the original Z_{DR} estimates in Figure 5 (b). Also, differential phase was artificially set to 0º at the beginning of the interval. To simulate coupling, original time-series are mixed as in (7) where we took that F_{hh} = F_{vv} = 1 and F_{hv} = F_{vh} in case when CPS is 40 dB. We set γ_{hv} = γ_{vh} = γ to 90° because (30) shows that is where the bias peak occurs for Φ_{DP} of zero. In case when CPS is 25 dB, we set $|F_{hv}|$ = $|F_{vh}|$ and γ_{hv} = 90º, γ_{vh} = 0º as the maximum bias occurs for those values if Φ_{DP} = 0º. In both cases we set β = 0º.

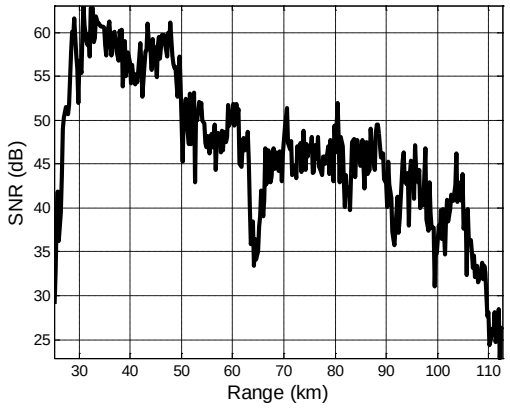

(a)

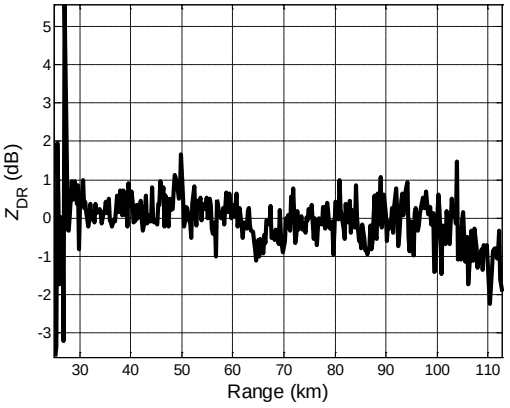

(b)

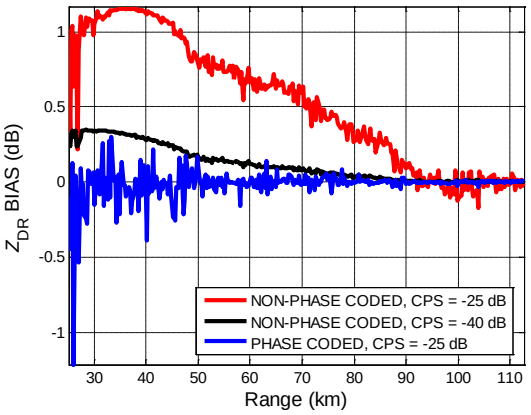

(c)

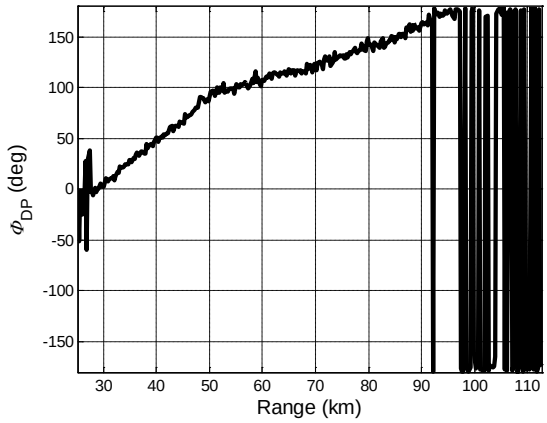

(d)

Figure 5. Assessment of Z_{DR} bias using real time-series for M = 16.

Next test is similar to previous except that we take the time-series to be the same in both channels. Results are presented in Figure 6.

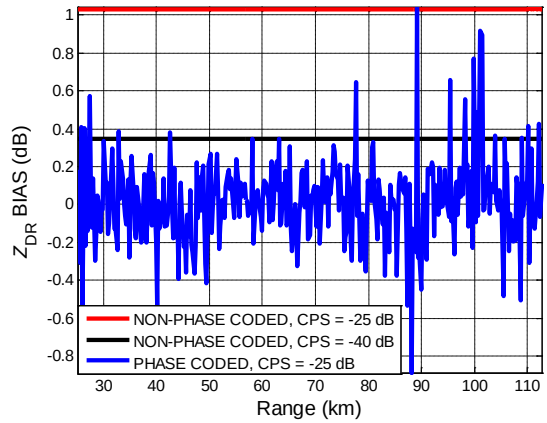

Figure 6. Assessment of Z_{DR} bias using real time-series only from H channel for M = 17.

Next we assess the behavior of the correlation coefficient estimates using simulation. Results are presented in Figure 7. Figure 7 (a) shows that the bias is within the acceptable limits of 0.01 when phase coding is not applied. Unfortunately, Figure 7 (b) implies that if phase coding is applied the bias exceeds that limit for a range of γ_{hv}, and γ_{vh} values. Phase coding does seem to reduce overall variance somewhat compared to the non-phase coded data. For reference, the bias and standard deviation of the non-coupled data are 5.8×10^{-5} and 6.2×10^{-3}.

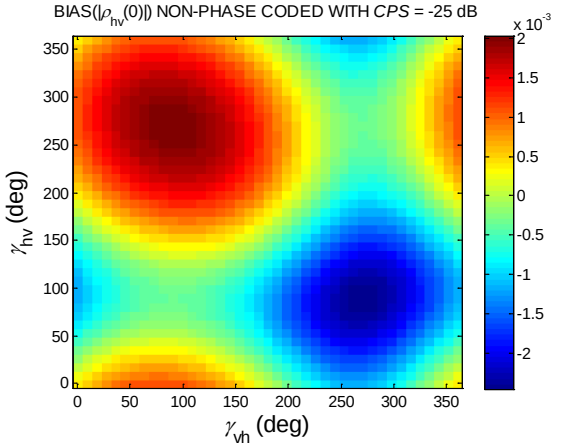

(a)

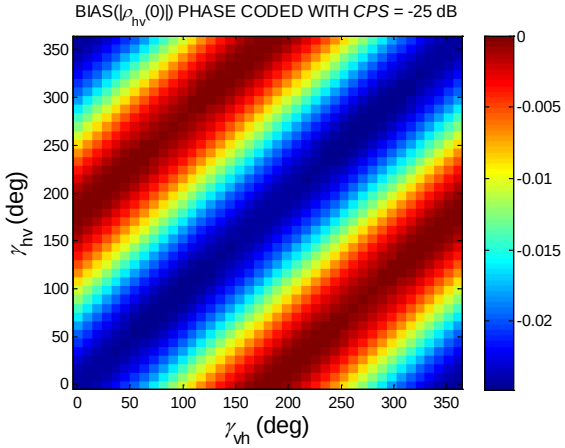

(b)

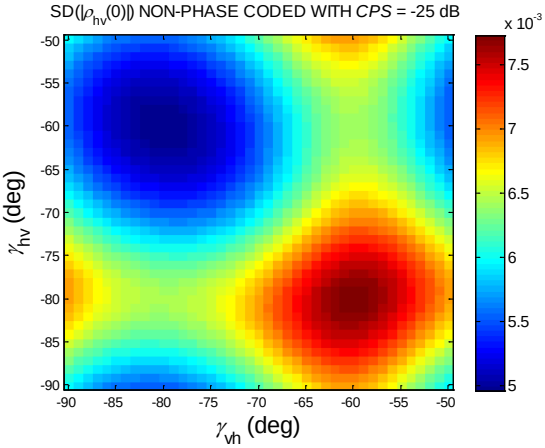

(c)

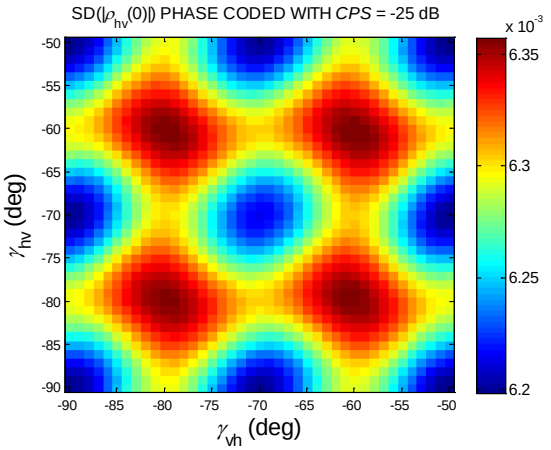

(d)

Figure 7. Correlation coefficient biases and standard deviations for non-phase coded and phase coded simulated data with M = 16, SNR = 50 dB, σ_V = 2 m s^{-1}, Z_{DR} = 0 dB, $|\rho_{hv}(0)|$ = 0.99, Φ_{DP} = 0°, and LDR = -Inf dB.

4. SUMMARY

In this work the use of pulse to pulse phase codes to improve the cross-polar isolation was investigated. It is shown that such phase codes have the potential to reduce the cross-polar contamination and thus reduce the differential reflectivity bias so that it falls within acceptable limits. At the same time, these codes have no adverse effects on the standard deviations of the differential reflectivity. It is concluded, however, that these phase codes can have adverse effect on the correlation coefficient bias by increasing it to values that are beyond the acceptable ones.

ACKNOWLEDGEMENT

This conference paper was prepared with funding provided by NOAA/Office of Oceanic and Atmospheric Research under NOAA-University of Oklahoma Cooperative Agreement #NA11OAR4320072, U.S. Department of Commerce. The statements, findings, conclusions, and recommendations are those of the author(s) and do not necessarily reflect the views of NOAA or the U.S. Department of Commerce.

REFERENCES

Chandrasekhar, V., and N. Bharadwaj, 2009: Orthogonal Channel Coding for Simultaneous Co- and Cross-Polarization Measurements. J. Atmos. Oceanic Technol., **26,** 45-56.

Doviak, R.J., and D.S. Zrnić, 1993: *Doppler radar and weather observations*. Academic Press, 562 pp.

D. Giuli, M. Fossi, and L. Facheris, 1993: Radar target scattering matrix measurement through orthogonal signals, *IEE Proceedings-F*, **140**, No. 4, pp. 233 – 242.

Heinselman, P.M., and S.M. Torres, 2011: High-Temporal-Resolution Capabilities of the National Weather Radar Testbed Phased-Array Radar. *J. Applied Meteor. Climat.,* **50,** 579-593.

Knapp, E.J, J.Salazar, R.H. Medina, A. Krishnamurthy, and R. Tessier, 2011: Phase-tilt radar antenna array. European Microwave Conference 2011. *J. Atmos. Oceanic Technol.,*

Melnikov V.M,, and D.S. Zrnić, 2007: Autocorrelation and Cross-Correlation Estimators of Polarimetric Variables, J. Atmos. Oceanic Technol., **24,** 1337-1350.

Ryzhkov, A. V., 2001: Interpretation of Polarimetric Radar Covariance Matrix for Meteorological Scatterers: Theoretical Analysis. *J. Atmos. Oceanic Technol.,* **18**, 315-328

Sachidananda, M., and D. S. Zrnić, 1985: Z_{DR} measurement considerations for a fast scan capability radar. Radio Sci., 20, 907–922.

Sachidananda, M., and D.S. Zrnić, 1986: Recovery of Spectral Moments from Overlaid Echoes in a Doppler Weather Radar. *IEEE Trans. Geosci. Remote Sens.*, **GE-24**, pp. 751-764.

Stagliano, J.J., J.L. Alford, J.R. Hevlin, and D.A. Nelson, 2009: Phase shifted transmitted signals in a simultaneous dual polarization weather system. US patent No.7,551,1232 B2.

Stagliano, J. J., R. J. Helvin, L. J. Alford, and D. Nelson, 2006: Measuring the linear depolarization ratio simultaneously with the other polarimetric variables. Proc. Fourth European Conf. on Radar in Meteorology and Hydrology, Barcelona, Spain, Servei Meteorologic de Catalunya, 80–83.

Torres S. M., 2001: Estimation of Doppler and Polarimetric Variables for Weather Radars, Ph.D. dissertation, The University of Oklahoma, Norman, OK.

Weadon,M., P. Heinselman, D. Forsyth, W. E. Benner, G. S. Torok, and J. Kimpel, 2009: Multifunction Phased Array Radar. *Bulletin of the American Meteorological Society (BAMS)*, pp. 385-389.

Zhang, G., R.J. Doviak, D. Zrnić, J. Crain, D. Staiman, and Yasser Al-Rashid, 2009: Phased Array Radar Polarimetry for Weather Sensing: A Theoretical Formulation for Bias Corrections. *IEEE Trans. Geosci. Remote Sens.,* **47,** 3679-3689.

Zhang, G., R. J. Doviak, D. S. Zrnić, R. Palmer, L. Lei, and Y. Al-Rashid, 2011: Polarimetric Phased Array Radar for Weather Measurement: A Planar or Cylindrical Configuration? *J. Atmos. Oceanic Technol.,* **28,** 63-73.

Zrnić D.S., 1975: Simulation of weather like Doppler spectra and signals, *J. Appl. Meteorol*., 619-620.

Zrnić, D. S., J. F. Kimpel, D. E. Forsyth, A. Shapiro, G. Crain, R. Ferek, J. Heimmer, W. Benner, T.J. McNellis, R.J. Vogt, 2007: Agile beam phased array

radar for weather observations. *Bull. Amer. Meteor. Soc.*, **88**, 1753-1766

Zrnić, D.S., R.J. Doviak, G. Zhang, and R.V. Ryzhkov, 2010: Bias in differential reflectivity due to cross-coupling through the radiation patterns of polarimetric weather radars. *J. Atmos. Oceanic Technol*., **27**, 1624-1637.

Zrnić, D.S., R.J. Doviak, V.M. Melnikov, and I.R. Ivić, 2013: Signal design to suppress coupling in the SHV polarimetric mode. Submitted to *J. Atmos. Oceanic Technol*.

APPENDIX A

In this appendix we derive the expressions for $\delta P_h(m)$ and $\delta P_v(m)$ (i.e., bias inducing terms in the H and V power estimates) shown in (9). These can be represented as

$$\begin{aligned}\delta P_h(m) &= 2\mathrm{Re}\left\{F_{hh}^2 s_{hh}^*(m)\Delta_h(m)\right\} \\ &\quad + \left|\Delta_h(m)\right|^2 \\ \delta P_v(m) &= 2\mathrm{Re}\left\{F_{vv}^2 s_{vv}^*(m)e^{-j\beta}\Delta_v(m)\right\} \\ &\quad + \left|\Delta_v(m)\right|^2\end{aligned} \tag{A.1}$$

where

$$\begin{aligned}\Delta_h(m) &= F_{vh}^2 s_{vv}(m) + 2F_{hh}F_{vh}s_{hv}(m) + \\ &\left[F_{hh}F_{hv}s_{hh}(m) + F_{vv}F_{vh}s_{vv}(m) + \right. \\ &\left.\left(F_{hh}F_{vv} + F_{hv}F_{vh}\right)s_{hv}(m)\right]e^{j(\beta+\alpha_v(m)-\alpha_h(m))} \\ \Delta_v(m) &= F_{hv}^2 s_{hh}(m)e^{j\beta} + 2F_{vv}F_{hv}e^{j\beta}s_{hv}(m) + \\ &\left[F_{vv}F_{vh}s_{vv}(m) + F_{hh}F_{hv}s_{hh}(m) + \right. \\ &\left.\left(F_{hh}F_{vv} + F_{hv}F_{vh}\right)s_{hv}(m)\right]e^{j(\alpha_h(m)-\alpha_v(m))}\end{aligned} \tag{A.2}$$

Without the loss of generality we can assume that

$$\begin{aligned}&\int_\Omega \left|\Delta_h(m)\right|^2 d\Omega \approx \int_\Omega \left(F_{hh}^2F_{vv}^2\left|s_{hv}(m)\right|^2 + \right. \\ &F_{hh}^2\left|F_{hv}\right|^2\left|s_{hh}(m)\right|^2 + F_{vv}^2\left|F_{vh}\right|^2\left|s_{vv}(m)\right|^2 + \\ &2\mathrm{Re}\left\{F_{hh}F_{vv}F_{hv}^*F_{vh}s_{hh}^*(m)s_{vv}(m) + \right. \\ &F_{vv}^2F_{hh}F_{vh}^*s_{vv}^*(m)s_{hv}(m) + \\ &F_{hh}^2F_{vv}F_{hv}^*s_{hh}^*(m)s_{hv}(m) + \\ &\left.\left.2F_{vv}^2F_{hh}F_{hv}^*\left|s_{hv}(m)\right|^2 e^{-j(\beta+\alpha_v(m)-\alpha_h(m))}\right\}\right)d\Omega\end{aligned}$$

$$\begin{aligned}&\int_\Omega \left|\Delta_v(m)\right|^2 d\Omega \approx \int_\Omega \left(F_{hh}^2F_{vv}^2\left|s_{hv}(m)\right|^2 + \right. \\ &F_{hh}^2\left|F_{hv}\right|^2\left|s_{hh}(m)\right|^2 + F_{vv}^2\left|F_{vh}\right|^2\left|s_{vv}(m)\right|^2 + \\ &2\mathrm{Re}\left\{F_{hh}F_{vv}F_{hv}^*F_{vh}s_{hh}^*(m)s_{vv}(m) + \right. \\ &F_{vv}^2F_{hh}F_{vh}^*s_{vv}^*(m)s_{hv}(m) + \\ &F_{hh}^2F_{vv}F_{hv}^*s_{hh}^*(m)s_{hv}(m) + \\ &\left.\left.2F_{vv}^2F_{hh}F_{hv}^*\left|s_{hv}(m)\right|^2 e^{-j(\beta+\alpha_v(m)-\alpha_h(m))}\right\}\right)d\Omega\end{aligned} \tag{A.3}$$

Also,

$$\begin{aligned}&\int_\Omega 2\mathrm{Re}\left\{F_{hh}^2 s_{hh}^*(m)\Delta_h(m)\right\}d\Omega = \\ &2\int_\Omega \mathrm{Re}\left\{F_{hh}^2F_{vh}^2 s_{hh}^*(m)s_{vv}(m) + \right. \\ &2F_{hh}^3F_{vh}s_{hh}^*(m)s_{hv}(m) + \\ &\left(F_{hh}^3F_{hv}\left|s_{hh}(m)\right|^2 + F_{hh}^2F_{vv}F_{vh}s_{hh}^*(m)s_{vv}(m) + \right. \\ &F_{hh}^2\left[F_{hh}F_{vv} + F_{hv}F_{vh}\right]s_{hh}^*(m)s_{hv}(m)\big)\times \\ &\left.e^{j(\beta+\alpha_v(m)-\alpha_h(m))}\right\}d\Omega \\ &\int_\Omega 2\mathrm{Re}\left\{F_{vv}^2 s_{vv}^*(m)e^{-j\beta}\Delta_v(m)\right\}d\Omega = \\ &2\int_\Omega \mathrm{Re}\left\{F_{vv}^2F_{hv}^2 s_{vv}^*(m)s_{hh}(m) + \right. \\ &2F_{vv}^3F_{hv}s_{vv}^*(m)s_{hv}(m) + \\ &\left(F_{vv}^3F_{vh}\left|s_{vv}(m)\right|^2 + F_{vv}^2F_{hh}F_{hv}s_{vv}^*(m)s_{hh}(m) + \right. \\ &F_{vv}^2\left[F_{hh}F_{vv} + F_{hv}F_{vh}\right]s_{vv}^*(m)s_{hv}(m)\big)\times \\ &\left.e^{j(-\beta+\alpha_h(m)-\alpha_v(m))}\right\}d\Omega\end{aligned} \tag{A.4}$$

Then, we represent the bias terms as

$$\begin{aligned}\delta P_h(m) &\approx \int_\Omega \left[A_h(m) + \right. \\ &\left.2\mathrm{Re}\left\{B_h(m)e^{j(\beta+\alpha_v(m)-\alpha_h(m))}\right\}\right]d\Omega \\ \delta P_v(m) &\approx \int_\Omega \left[A_v(m) + \right. \\ &\left.2\mathrm{Re}\left\{B_v(m)e^{-j(\beta+\alpha_v(m)-\alpha_h(m))}\right\}\right]d\Omega\end{aligned} \tag{A.5}$$

where

$$
\begin{aligned}
A_h(m) &= F_{hh}^2 F_{vv}^2 \left|s_{hv}(m)\right|^2 + \\
&F_{hh}^2 \left|F_{hv}\right|^2 \left|s_{hh}(m)\right|^2 + F_{vv}^2 \left|F_{vh}\right|^2 \left|s_{vv}(m)\right|^2 + \\
&2\mathrm{Re}\left\{F_{hh}F_{vv}F_{hv}^* F_{vh} s_{hh}^*(m) s_{vv}(m) + \right. \\
&F_{hh}^2 F_{vh}^2 s_{hh}^*(m) s_{vv}(m) + \\
&F_{hh}^2 F_{vv}F_{hv}^* s_{hh}^*(m) s_{hv}(m) + \\
&F_{vv}^2 F_{hh}F_{vh}^* s_{vv}^*(m) s_{hv}(m) + \\
&\left. 2F_{hh}^3 F_{vh} s_{hh}^*(m) s_{hv}(m)\right\}
\end{aligned}
$$

$$
\begin{aligned}
B_h(m) &= 2F_{hh}^2 F_{vv}F_{vh}^* \left|s_{hv}(m)\right|^2 + \\
&F_{hh}^3 F_{vv} s_{hh}^*(m) s_{hv}(m) + \\
&F_{hh}^3 F_{hv} \left|s_{hh}(m)\right|^2 + F_{hh}^2 F_{vv}F_{vh} s_{hh}^*(m) s_{vv}(m)
\end{aligned}
$$

$$
\begin{aligned}
A_v(m) &= F_{vv}^2 F_{hh}^2 \left|s_{hv}(m)\right|^2 + \\
&F_{hh}^2 \left|F_{hv}\right|^2 \left|s_{hh}(m)\right|^2 + F_{vv}^2 \left|F_{vh}\right|^2 \left|s_{vv}(m)\right|^2 + \\
&2\mathrm{Re}\left\{F_{hh}F_{vv}F_{vh}^* F_{hv} s_{vv}^*(m) s_{hh}(m) + \right. \\
&F_{vv}^2 F_{hv}^2 s_{vv}^*(m) s_{hh}(m) + \\
&F_{vv}^2 F_{hh}F_{vh}^* s_{vv}^*(m) s_{hv}(m) + \\
&F_{hh}^2 F_{vv}F_{hv}^* s_{hh}^*(m) s_{hv}(m) + \\
&\left. 2F_{vv}^3 F_{hv} s_{vv}^*(m) s_{hv}(m)\right\}
\end{aligned}
\tag{A.6}
$$

$$
\begin{aligned}
B_v(m) &= 2F_{vv}^2 F_{hh}F_{hv}^* \left|s_{hv}(m)\right|^2 + \\
&F_{vv}^3 F_{hh} s_{vv}^*(m) s_{hv}(m) + \\
&F_{vv}^3 F_{vh} \left|s_{vv}(m)\right|^2 + F_{vv}^2 F_{hh}F_{hv} s_{vv}^*(m) s_{hh}(m)
\end{aligned}
$$

Note that the phase codes bear no impact on the $A_h(m)$ and $A_v(m)$ in (A.5) and that these are caused by the depolarization in the scattering media. The expected values of the terms in are

$$
\begin{aligned}
\left\langle A_h(m)\right\rangle &= \left\langle \left|s_{hh}(m)\right|^2 \right\rangle \left(F_{hh}^2 F_{vv}^2 LDR + \right. \\
&F_{hh}^2 \left|F_{hv}\right|^2 + \frac{F_{vv}^2 \left|F_{vh}\right|^2}{Z_{dr}} + \\
&2\mathrm{Re}\left\{\left(F_{hh}F_{vv}F_{hv}^* F_{vh} + F_{hh}^2 F_{vh}^2\right) \frac{\left|\rho_{hv}(0)\right| e^{j\Phi_{DP}}}{\sqrt{Z_{dr}}} + \right. \\
&\left(F_{hh}^2 F_{vv}F_{hv}^* + 2F_{hh}^3 F_{vh}\right) \rho_{xh} \sqrt{LDR} e^{j\frac{\Phi_{DP}}{2}} + \\
&\left.\left. F_{vv}^2 F_{hh}F_{vh}^* \rho_{xv} \sqrt{\frac{LDR}{Z_{dr}}} e^{-j\frac{\Phi_{DP}}{2}} \right\}\right)
\end{aligned}
$$

$$
\begin{aligned}
\left\langle B_h(m)\right\rangle &= \left\langle \left|s_{hh}(m)\right|^2 \right\rangle \left[2F_{hh}^2 F_{vv}F_{vh}^* LDR + \right. \\
&F_{hh}^3 F_{vv} \rho_{xh} \sqrt{LDR} e^{j\frac{\Phi_{DP}}{2}} + F_{hh}^3 F_{hv} + \\
&\left. F_{hh}^2 F_{vv}F_{vh} \frac{\left|\rho_{hv}(0)\right|}{\sqrt{Z_{dr}}} e^{j\Phi_{DP}} \right]
\end{aligned}
\tag{A.7}
$$

$$
\begin{aligned}
\left\langle A_v(m)\right\rangle &= \left\langle \left|s_{vv}(m)\right|^2 \right\rangle \left(F_{hh}^2 F_{vv}^2 Z_{dr} LDR + \right. \\
&F_{hh}^2 \left|F_{vh}\right|^2 + F_{vv}^2 \left|F_{hv}\right|^2 Z_{dr} + \\
&2\mathrm{Re}\left\{\left(F_{hh}F_{vv}F_{vh}^* F_{hv} + F_{vv}^2 F_{hv}^2\right) \sqrt{Z_{dr}} \left|\rho_{hv}(0)\right| e^{-j\Phi_{DP}} + \right. \\
&\left(F_{vv}^2 F_{hh}F_{vh}^* + 2F_{vv}^3 F_{hv}\right) \rho_{xv} \sqrt{Z_{dr}} \sqrt{LDR} e^{-j\frac{\Phi_{DP}}{2}} + \\
&\left.\left. F_{hh}^2 F_{vv}F_{hv}^* \rho_{xh} Z_{dr} \sqrt{LDR} e^{j\frac{\Phi_{DP}}{2}} \right\}\right)
\end{aligned}
$$

$$
\begin{aligned}
\left\langle B_v(m)\right\rangle &= \left\langle \left|s_{vv}(m)\right|^2 \right\rangle \left[2F_{vv}^2 F_{hh}F_{hv}^* Z_{dr} LDR + \right. \\
&F_{vv}^3 F_{hh} \rho_{xv} \sqrt{Z_{dr}} \sqrt{LDR} e^{-j\frac{\Phi_{DP}}{2}} + F_{vv}^3 F_{vh} + \\
&\left. F_{vv}^2 F_{hh}F_{hv} \left|\rho_{hv}(0)\right| \sqrt{Z_{dr}} e^{-j\Phi_{DP}} \right]
\end{aligned}
$$

In view of assumptions we obtain after integrating (A.5)

$$
\begin{aligned}
\delta P_h'(m) &\approx A_h'(m) + \\
&\quad 2\mathrm{Re}\left\{B_h'(m) e^{j(\beta + \alpha_v(m) - \alpha_h(m))}\right\} \\
\delta P_v'(m) &\approx A_v'(m) + \\
&\quad 2\mathrm{Re}\left\{B_v'(m) e^{-j(\beta + \alpha_v(m) - \alpha_h(m))}\right\}
\end{aligned}
\tag{A.8}
$$

where the expected values of the terms in are

$$\left\langle A_h'(m)\right\rangle = g^2 S_h \left[LDR + CPS\left(1+\frac{1}{Z_{dr}}\right) + 2\mathrm{Re}\left\{ \sqrt{CPS}e^{-j\gamma_{vh}}\rho_{xv}\sqrt{\frac{LDR}{Z_{dr}}}e^{-j\frac{\Phi_{DP}}{2}} + \sqrt{CPS}\left(e^{-j\gamma_{hv}}+2e^{j\gamma_{vh}}\right)\rho_{xh}\sqrt{LDR}e^{j\frac{\Phi_{DP}}{2}} + CPS\left(e^{j(\gamma_{vh}-\gamma_{hv})}+e^{j2\gamma_{vh}}\right)\frac{\left|\rho_{hv}(0)\right|e^{j\Phi_{DP}}}{\sqrt{Z_{dr}}}\right\}\right]$$

$$\left\langle B_h'(m)\right\rangle = g^2 S_h \left[2\sqrt{CPS}e^{-j\gamma_{vh}}LDR + \rho_{xh}\sqrt{LDR}e^{j\frac{\Phi_{DP}}{2}} + \sqrt{CPS}e^{j\gamma_{hv}} + \sqrt{CPS}e^{j\gamma_{vh}}\frac{\left|\rho_{hv}(0)\right|}{\sqrt{Z_{dr}}}e^{j\Phi_{DP}}\right] \quad \text{(A.9)}$$

$$\left\langle A_v'(m)\right\rangle = g^2 S_v \left[Z_{dr}LDR + CPS\left(1+Z_{dr}\right) + 2\mathrm{Re}\left\{ \sqrt{CPS}e^{-j\gamma_{hv}}\rho_{xh}Z_{dr}\sqrt{LDR}e^{j\frac{\Phi_{DP}}{2}} + \sqrt{CPS}\left(e^{-j\gamma_{vh}}+2e^{j\gamma_{hv}}\right)\rho_{xv}\sqrt{Z_{dr}}\sqrt{LDR}e^{-j\frac{\Phi_{DP}}{2}} + CPS\left(e^{j(\gamma_{hv}-\gamma_{vh})}+e^{j2\gamma_{hv}}\right)\sqrt{Z_{dr}}\left|\rho_{hv}(0)\right|e^{-j\Phi_{DP}}\right\}\right]$$

$$\left\langle B_v'(m)\right\rangle = g^2 S_v \left[2\sqrt{CPS}e^{-j\gamma_{hv}}Z_{dr}LDR + \rho_{xv}\sqrt{Z_{dr}}\sqrt{LDR}e^{-j\frac{\Phi_{DP}}{2}} + \sqrt{CPS}e^{j\gamma_{vh}} + \sqrt{CPS}e^{j\gamma_{hv}}\left|\rho_{hv}(0)\right|\sqrt{Z_{dr}}e^{-j\Phi_{DP}}\right]$$

APPENDIX B

Let's see what happens when we sum two consecutive terms in (11). Note that the mathematical expectations of $A_c(m)$ and $B_c(m)$ (c is h or v) are the same for every m because we assume them to be wide-sense stationary random variables. We get

$$\begin{aligned}
&\left\langle \hat{P}_h(m)\right\rangle + \left\langle \hat{P}_h(m+1)\right\rangle \approx 2\int_\Omega \left[F_{hh}^4 \left\langle \left|s_{hh}(m)\right|^2\right\rangle + \left\langle A_h(m)\right\rangle + 2\mathrm{Re}\left\{\left\langle B_h(m)\right\rangle e^{j\beta}\times \left(e^{j(\alpha_v(m)-\alpha_h(m))}+e^{j(\alpha_v(m+1)-\alpha_h(m+1))}\right)\right\}\right] d\Omega \\
&\left\langle \hat{P}_v(m)\right\rangle + \left\langle \hat{P}_v(m+1)\right\rangle \approx 2\int_\Omega \left[F_{vv}^4 \left\langle \left|s_{vv}(m)\right|^2\right\rangle + \left\langle A_v(m)\right\rangle + 2\mathrm{Re}\left\{\left\langle B_v(m)\right\rangle e^{-j\beta}\times \left(e^{-j(\alpha_v(m)-\alpha_h(m))}+e^{-j(\alpha_v(m+1)-\alpha_h(m+1))}\right)\right\}\right] d\Omega
\end{aligned} \quad \text{(B.1)}$$

Hence, in H the bias inducing term, affected by the phase codes, can be represented as

$$\begin{aligned}
&\left\langle \left|B_h(m)\right|\right\rangle \left[\cos\left(\alpha_B+\beta+\alpha_v(m)-\alpha_h(m)\right)+\cos\left(\alpha_B+\beta+\alpha_v(m+1)-\alpha_h(m+1)\right)\right] = \\
&\left\langle \left|B_h(m)\right|\right\rangle \left[\cos(\alpha_B+\beta)\cos\left(\alpha_v(m)-\alpha_h(m)\right)-\sin(\alpha_B+\beta)\sin\left(\alpha_v(m)-\alpha_h(m)\right)+\cos(\alpha_B+\beta)\cos\left(\alpha_v(m+1)-\alpha_h(m+1)\right)-\sin(\alpha_B+\beta)\sin\left(\alpha_v(m+1)-\alpha_h(m+1)\right)\right]
\end{aligned} \quad \text{(B.2)}$$

where

$$\alpha_B = \arg\left(\left\langle \left|B_h(m)\right|\right\rangle\right) \quad \text{(B.3)}$$

Similar can be shown for V as

$$\begin{aligned}
&\left\langle \left|B_v(m)\right|\right\rangle \left[\cos(\alpha_B+\beta)\cos\left(\alpha_h(m)-\alpha_v(m)\right)-\sin(\alpha_B+\beta)\sin\left(\alpha_h(m)-\alpha_v(m)\right)+\cos(\alpha_B+\beta)\cos\left(\alpha_h(m+1)-\alpha_v(m+1)\right)-\sin(\alpha_B+\beta)\sin\left(\alpha_h(m+1)-\alpha_v(m+1)\right)\right]
\end{aligned} \quad \text{(B.4)}$$

where

$$\alpha_B = \arg\left(\left\langle \left|B_v(m)\right|\right\rangle\right) \quad \text{(B.5)}$$

APPENDIX C

The product of samples from H and V is

$$
\begin{aligned}
&V_h^*(m)V_v(m) \sim \int_\Omega \Big[F_{hh}^2 F_{vv}^2 s_{hh}^*(m) s_{vv}(m) e^{j\beta} + \\
&2F_{hh}^2 F_{vv} F_{hv} e^{j\beta} s_{hh}^*(m) s_{hv}(m) + \\
&2F_{vv}^2 F_{hh} F_{vh}^* e^{j\beta} s_{vv}(m) s_{hv}^*(m) + \\
&\Big[F_{hh}^3 F_{hv} |s_{hh}(m)|^2 + F_{hh}^3 F_{vv} s_{hh}^*(m) s_{hv}(m) + \\
&F_{hh}^2 F_{vv} F_{vh} s_{hh}^*(m) s_{vv}(m) + 2F_{hh}^2 F_{vv} F_{vh}^* |s_{hv}(m)|^2 + \\
&F_{vv}^3 F_{vh}^* |s_{vv}(m)|^2 + F_{vv}^3 F_{hh} s_{vv}(m) s_{hv}^*(m) + \\
&F_{vv}^2 F_{hh} F_{hv}^* s_{hh}^*(m) s_{vv}(m) + \\
&2F_{vv}^2 F_{hh} F_{hv} |s_{hv}(m)|^2 \Big] e^{j(\alpha_h(m)-\alpha_v(m))} + \\
&\Big[F_{hh}^2 F_{vv}^2 |s_{hv}(m)|^2 + \\
&2\mathrm{Re}\left\{ F_{vv}^2 F_{hh} F_{vh}^* s_{vv}^*(m) s_{hv}(m) + \right. \\
&\left. F_{hh}^2 F_{vv} F_{hv}^* s_{hh}^*(m) s_{hv}(m) \right\} \Big] e^{-j\beta} e^{j2(\alpha_h(m)-\alpha_v(m))} \Big] d\Omega
\end{aligned}
\tag{C.1}
$$

where we assume $\exp(j\psi_h(\Theta, \varphi)) = \exp(j\psi_v(\Theta, \varphi))$. Now,

$$
\begin{aligned}
&\left\langle V_h^*(m)V_v(m) \right\rangle + \left\langle V_h^*(m+1)V_v(m+1) \right\rangle \sim \\
&2\int_\Omega \Big\{ F_{hh}^2 F_{vv}^2 \left\langle s_{hh}^*(m) s_{vv}(m) \right\rangle e^{j\beta} + \\
&2F_{hh}^2 F_{vv} F_{hv} e^{j\beta} \left\langle s_{hh}^*(m) s_{hv}(m) \right\rangle + \\
&2F_{vv}^2 F_{hh} F_{vh}^* e^{j\beta} \left\langle s_{vv}(m) s_{hv}^*(m) \right\rangle + \\
&\Big[F_{hh}^3 F_{hv} \left\langle |s_{hh}(m)|^2 \right\rangle + F_{hh}^3 F_{vv} \left\langle s_{hh}^*(m) s_{hv}(m) \right\rangle + \\
&F_{hh}^2 F_{vv} F_{vh} \left\langle s_{hh}^*(m) s_{vv}(m) \right\rangle + \\
&2F_{hh}^2 F_{vv} F_{vh}^* \left\langle |s_{hv}(m)|^2 \right\rangle + \\
&F_{vv}^3 F_{vh}^* \left\langle |s_{vv}(m)|^2 \right\rangle + F_{vv}^3 F_{hh} \left\langle s_{vv}(m) s_{hv}^*(m) \right\rangle + \\
&F_{vv}^2 F_{hh} F_{hv}^* \left\langle s_{hh}^*(m) s_{vv}(m) \right\rangle + \\
&2F_{vv}^2 F_{hh} F_{hv} \left\langle |s_{hv}(m)|^2 \right\rangle \Big] \times \\
&\left(e^{j(\alpha_h(m)-\alpha_v(m))} + e^{j(\alpha_h(m+1)-\alpha_v(m+1))} \right) + \\
&\Big[F_{hh}^2 F_{vv}^2 \left\langle |s_{hv}(m)|^2 \right\rangle + \\
&2\mathrm{Re}\left\{ F_{vv}^2 F_{hh} F_{vh}^* \left\langle s_{vv}^*(m) s_{hv}(m) \right\rangle + \right. \\
&\left. F_{hh}^2 F_{vv} F_{hv}^* \left\langle s_{hh}^*(m) s_{hv}(m) \right\rangle \right\} \Big] e^{-j\beta} \times \\
&\left(e^{j2(\alpha_h(m)-\alpha_v(m))} + e^{j2(\alpha_h(m+1)-\alpha_v(m+1))} \right) \Big\} d\Omega
\end{aligned}
\tag{C.2}
$$

If any of the conditions in (15) is met then

$$
\begin{aligned}
e^{j(\alpha_h(m)-\alpha_v(m))} + e^{j(\alpha_h(m+1)-\alpha_v(m+1))} &= 0 \\
e^{j2(\alpha_h(m)-\alpha_v(m))} + e^{j2(\alpha_h(m+1)-\alpha_v(m+1))} &= 2e^{-j2\alpha}
\end{aligned}
\tag{C.3}
$$

This produces

$$
\begin{aligned}
&\left\langle V_h^*(m)V_v(m) \right\rangle + \left\langle V_h^*(m+1)V_v(m+1) \right\rangle \sim \\
&2\int_\Omega \Big\{ F_{hh}^2 F_{vv}^2 \left\langle s_{hh}^*(m) s_{vv}(m) \right\rangle e^{j\beta} + \\
&2F_{hh}^2 F_{vv} F_{hv} e^{j\beta} \left\langle s_{hh}^*(m) s_{hv}(m) \right\rangle + \\
&2F_{vv}^2 F_{hh} F_{vh}^* e^{j\beta} \left\langle s_{vv}(m) s_{hv}^*(m) \right\rangle + \\
&2\Big[F_{hh}^2 F_{vv}^2 \left\langle |s_{hv}(m)|^2 \right\rangle + \\
&2\mathrm{Re}\left\{ F_{vv}^2 F_{hh} F_{vh}^* \left\langle s_{vv}^*(m) s_{hv}(m) \right\rangle + \right. \\
&\left. F_{hh}^2 F_{vv} F_{hv}^* \left\langle s_{hh}^*(m) s_{hv}(m) \right\rangle \right\} \Big] e^{-j(\beta+\alpha)} \Big\} d\Omega
\end{aligned}
\tag{C.4}
$$

APPENDIX D

To simulate samples of $s_{hv}(m)$ we follow similar procedure as in Torres 2001. We have samples of $s_{hh}(m)$ that are produced as

$$
s_{hh}(m) = \left\langle |s_{hh}(m)|^2 \right\rangle X(m) e^{-j\Phi_{DP}} \tag{D.1}
$$

Where $X(m)$ are unit power Gaussian distributed samples with desired autocorrelation in sample-time. Next, we need to construct $s_{hv}(m)$ so that

$$
\begin{aligned}
LDR &= \frac{\left\langle |s_{hv}(m)|^2 \right\rangle}{\left\langle |s_{hh}(m)|^2 \right\rangle} \\
\rho_{xh} e^{j\frac{\Phi_{DP}}{2}} &= \frac{\left\langle s_{hh}^*(m) s_{hv}(m) \right\rangle}{\sqrt{\left\langle |s_{hh}(m)|^2 \right\rangle \left\langle |s_{hv}(m)|^2 \right\rangle}}
\end{aligned}
\tag{D.2}
$$

To achieve this we construct time series $X(m)$ with the same sample-time correlation as $s_{hh}(m)$ and unit power. Then

$$
s_{hv}(m) = A \frac{s_{hh}(m)}{\left\langle |s_{hh}(m)|^2 \right\rangle} + BY(m) \tag{D.3}
$$

where A and B are complex constants to be determined and $Y(m)$ are unit power Gaussian distributed samples with desired autocorrelation in sample-time independent of $X(m)$.

To obtain the desired autocorrelation in sample-time we have

$$
\begin{aligned}
R_{s_{hv}}(n) &= \left\langle s_{hv}^*(m) s_{hv}(m+n) \right\rangle \\
&= |A|^2 \rho_{s_{hh}}(n) + |B|^2 \rho_X(n) \\
&= \left(|A|^2 + |B|^2 \right) \rho_{s_{hh}}(n)
\end{aligned}
\tag{D.4}
$$

Clearly, one requirement is that

$$|A|^2 + |B|^2 = LDR\left\langle |s_{hh}(m)|^2 \right\rangle \tag{D.5}$$

Next,

$$\frac{\left\langle s_{hh}^*(m)s_{hv}(m)\right\rangle}{\sqrt{\left\langle |s_{hh}(m)|^2\right\rangle\left\langle |s_{hv}(m)|^2\right\rangle}} = \frac{A}{\left\langle |s_{hh}(m)|^2\right\rangle\sqrt{LDR}} = \rho_{xh}e^{j\frac{\Phi_{DP}}{2}} \tag{D.6}$$

Thus,

$$A = \rho_{xh}e^{j\frac{\Phi_{DP}}{2}}\left\langle |s_{hh}(m)|^2\right\rangle\sqrt{LDR} \tag{D.7}$$

Next, we solve for |B| as

$$|B| = \sqrt{LDR\left\langle |s_{hh}(m)|^2\right\rangle\left(1-|\rho_{xh}|^2\right)} \tag{D.8}$$

Note that the argument (phase) of *B* is not constrained to any particular value. If *B* is chosen to have the same argument as *A* then

$$\begin{aligned} s_{hv}(m) &= e^{j\left(\arg(\rho_{xh})+\frac{\Phi_{DP}}{2}\right)}\sqrt{LDR}\left(s_{hh}(m)|\rho_{xh}| + X(m)\sqrt{\left\langle |s_{hh}(m)|^2\right\rangle\left(1-|\rho_{xh}|^2\right)}\right) \\ &= e^{j\left(\arg(\rho_{xh})+\frac{\Phi_{DP}}{2}\right)}\sqrt{LDR\left\langle |s_{hh}(m)|^2\right\rangle}\times \\ &\left(\frac{s_{hh}(m)}{\sqrt{\left\langle |s_{hh}(m)|^2\right\rangle}}|\rho_{xh}| + X(m)\sqrt{\left(1-|\rho_{xh}|^2\right)}\right) \end{aligned} \tag{D.9}$$

Give n that $s_{vv}(m)$ is simulated as

$$s_{vv}(m) = \left[|\rho_{hv}(0)|\frac{s_{hh}(m)}{\sqrt{\left\langle |s_{hh}(m)|^2\right\rangle}}e^{j\Phi_{DP}} + \sqrt{1-|\rho_{hv}(0)|^2}Z(m)\right]\frac{\sqrt{\left\langle |s_{hh}(m)|^2\right\rangle}}{\sqrt{Z_{dr}}} \tag{D.10}$$

where $X(m)$ are unit power Gaussian distributed samples with desired autocorrelation in sample-time independent of $X(m)$ and $Y(m)$.The we get for ρ_{xv}

$$\begin{aligned} \rho_{xv}e^{-j\frac{\Phi_{DP}}{2}} &= \frac{\left\langle s_{vv}^*(m)s_{hv}(m)\right\rangle}{\sqrt{\left\langle |s_{vv}(m)|^2\right\rangle\left\langle |s_{hv}(m)|^2\right\rangle}} \\ &= |\rho_{hv}(0)|\sqrt{Z_{dr}}\rho_{xh}e^{-j\frac{\Phi_{DP}}{2}} \end{aligned} \tag{D.11}$$

$$\begin{aligned} \rho_{xh} &= \frac{\left\langle s_{hh}^*(m)s_{hv}(m)\right\rangle}{\sqrt{|s_{hh}(m)|^2|s_{hv}(m)|^2}} \\ \left\langle s_{hh}^*(m)s_{hv}(m)\right\rangle &= \rho_{xh}\sqrt{|s_{hh}(m)|^2|s_{hv}(m)|^2}e^{j\frac{\Phi_{DP}}{2}} \\ &= |s_{hh}(m)|^2\rho_{xh}\sqrt{LDR}e^{j\frac{\Phi_{DP}}{2}} \\ &= |s_{vv}(m)|^2 Z_{dr}\rho_{xh}\sqrt{LDR}e^{j\frac{\Phi_{DP}}{2}} \\ \rho_{xv} &= \frac{\left\langle s_{vv}^*(m)s_{hv}(m)\right\rangle}{\sqrt{|s_{vv}(m)|^2|s_{hv}(m)|^2}} \\ \left\langle s_{vv}^*(m)s_{hv}(m)\right\rangle &= \rho_{xv}\sqrt{|s_{vv}(m)|^2|s_{hv}(m)|^2}e^{-j\frac{\Phi_{DP}}{2}} \\ &= \rho_{xv}\sqrt{|s_{vv}(m)|^2|s_{hh}(m)|^2}\sqrt{LDR}e^{-j\frac{\Phi_{DP}}{2}} \\ &= |s_{hh}(m)|^2\rho_{xv}\frac{\sqrt{LDR}}{\sqrt{Z_{dr}}}e^{-j\frac{\Phi_{DP}}{2}} \\ &= |s_{vv}(m)|^2\rho_{xv}\sqrt{Z_{dr}}\sqrt{LDR}e^{-j\frac{\Phi_{DP}}{2}} \end{aligned} \tag{D.12}$$

APPENDIX E

In this appendix we study the variance of Z_{DR}. First we take

$$\hat{Z}_{DR}^2 \approx \left(\hat{Z}_{DR}^{NC}\right)^2 + \frac{20}{\ln(10)}\left(\frac{\hat{Z}_{DR}^{NC}\delta\hat{P}_h}{\hat{S}_h^{NC}} - \frac{\hat{Z}_{DR}^{NC}\delta\hat{P}_v}{\hat{S}_v^{NC}}\right) \tag{E.1}$$

where we consider only the terms that significantly contribute to the result. Given that

$$\left\langle \hat{Z}_{DR}\right\rangle^2 \approx \left\langle \hat{Z}_{DR}^{NC}\right\rangle^2 + \frac{20}{\ln(10)}\left(\frac{\left\langle \hat{Z}_{DR}^{NC}\right\rangle\left\langle \delta\hat{P}_h\right\rangle}{\left\langle \hat{S}_h^{NC}\right\rangle} - \frac{\left\langle \hat{Z}_{DR}^{NC}\right\rangle\left\langle \delta\hat{P}_v\right\rangle}{\left\langle \hat{S}_v^{NC}\right\rangle}\right) \tag{E.2}$$

We write

$$Var\left(\hat{Z}_{DR}\right) = Var\left(\hat{Z}_{DR}^{NC}\right) + \frac{20}{\ln(10)}\left(\left\langle\frac{\hat{Z}_{DR}^{NC}\delta\hat{P}_h}{\hat{S}_h^{NC}}\right\rangle - \frac{\left\langle \hat{Z}_{DR}^{NC}\right\rangle\left\langle \delta\hat{P}_h\right\rangle}{\left\langle \hat{S}_h^{NC}\right\rangle} - \left\langle\frac{\hat{Z}_{DR}^{NC}\delta\hat{P}_v}{\hat{S}_v^{NC}}\right\rangle + \frac{\left\langle \hat{Z}_{DR}^{NC}\right\rangle\left\langle \delta\hat{P}_v\right\rangle}{\left\langle \hat{S}_v^{NC}\right\rangle}\right) \tag{E.3}$$

Next we represent

$$\begin{aligned} \hat{Z}_{DR}^{NC} &= 10\log_{10}\left(\hat{S}_h\right) - 10\log_{10}\left(\hat{S}_v\right) \\ &\approx 10\log_{10}(S_h) + \frac{10\left(\hat{S}_h - S_h\right)}{\ln(10)S_h} - \\ &10\log_{10}(S_v) - \frac{10\left(\hat{S}_v - S_v\right)}{\ln(10)S_v} \end{aligned} \tag{E.4}$$

By plugging into we get

$$Var\left(\hat{Z}_{DR}\right) \approx Var\left(\hat{Z}_{DR}^{NC}\right) + \frac{200}{\ln^2(10)}\left\langle \frac{\delta\hat{P}_h}{S_h} - \frac{\hat{S}_v^{NC}\delta\hat{P}_h}{S_v\hat{S}_h^{NC}} + \frac{\delta\hat{P}_v}{S_v} - \frac{\hat{S}_h^{NC}\delta\hat{P}_v}{S_h\hat{S}_v^{NC}} \right\rangle \quad \text{(E.5)}$$

Using development into Taylor series we can write

$$\begin{aligned} \frac{\hat{S}_h^{NC}}{\hat{S}_v^{NC}} &\approx \frac{S_h}{S_v}\left(1 + \frac{\hat{S}_h^{NC}}{S_h} - \frac{\hat{S}_v^{NC}}{S_v}\right) \\ \frac{\hat{S}_v^{NC}}{\hat{S}_h^{NC}} &\approx \frac{S_v}{S_h}\left(1 - \frac{\hat{S}_h^{NC}}{S_h} + \frac{\hat{S}_v^{NC}}{S_v}\right) \end{aligned} \quad \text{(E.6)}$$

Then, after finding all the expected values we arrive at

$$\begin{aligned} &Var\left(\hat{Z}_{DR}\right) \approx Var\left(\hat{Z}_{DR}^{NC}\right) + \\ &g^2\frac{200}{\ln^2(10)}\left[CPS\left(2\frac{1-\left|\rho_{hv}(0)\right|^2}{M_I} + \right.\right. \\ &\left.\frac{\left|\rho_{hv}(0)\right|^2 - 1}{M_I}\left(Z_{dr} + \frac{1}{Z_{dr}}\right)\right) + \\ &2\sqrt{CPS}\frac{1-\left|\rho_{hv}(0)\right|^2}{M_I} \times \\ &\left.\left(\cos\left(\gamma_{hv} + \beta\right) + \cos\left(\gamma_{vh} - \beta\right)\right)\right] \end{aligned} \quad \text{(E.7)}$$

for the variance when no phase coding is applied.